

# Melting down a tetraquark: $D^*D^{(*)}$ interactions and $T_{cc}(3875)^+$ in a hot environment

V. Montesinos<sup>1,\*</sup>, G. Montana<sup>2,†</sup>, M. Albaladejo<sup>1,‡</sup>, J. Nieves<sup>1,§</sup> and L. Tolos<sup>3,4,¶</sup>

<sup>1</sup>*Instituto de Física Corpuscular (centro mixto CSIC-UV), Institutos de Investigación de Paterna, C/Catedrático José Beltrán 2, E-46980 Paterna, Valencia, Spain*

<sup>2</sup>*Theory Center, Thomas Jefferson National Accelerator Facility, Newport News, VA 23606, USA*

<sup>3</sup>*Institute of Space Sciences (ICE, CSIC), Campus UAB, Carrer de Can Magrans, 08193 Barcelona, Spain*

<sup>4</sup>*Institut d'Estudis Espacials de Catalunya (IEEC), 08860 Castelldefels (Barcelona), Spain*

We discuss the modification of the properties of the tetraquark-like  $T_{cc}(3875)^+$  and its heavy quark spin partner,  $T_{cc}(4016)^{++}$  immersed in a hot bath of pions. We consider these exotic states as purely isoscalar  $DD^*$  and  $D^*D^*$   $S$ -wave bound states, respectively. Finite temperature effects are incorporated through the  $D$  and  $D^*$  state-of-the-art thermal spectral functions calculated in [G. Montana *et al.*, *Phys. Rev. D*, **102** (2020) 096020], using the imaginary-time formalism. We find important modifications of the  $DD^*$  and  $D^*D^*$  scattering amplitudes already for  $T = 80$  MeV, and show that the hot-bath lineshapes of these tetraquark-like states strongly depend on their Weinberg molecular content. We find that the thermal  $T_{cc}(3875)^+$  and  $T_{cc}(4016)^{++}$  spectral functions change more rapidly with temperature for high molecular probabilities  $P_0$ . For large values of  $P_0$ , the widths significantly increase with temperature, leading to the melting of these exotic states for temperatures larger than 80 MeV. For small molecular components, the changes in the spectral functions of these states due to temperature become significantly less important. All these results show that any future experimental determination of the  $D^{(*)}D^*$  scattering amplitudes at finite temperature will provide valuable insights into the molecular content of the  $T_{cc}(3875)^+$  and  $T_{cc}(4016)^{++}$  exotics.

## I. INTRODUCTION

Since the beginning of the century, several new hadronic states have been experimentally determined. Starting from the pioneer discovery of the  $X(3872)$  in 2003 by the Belle Collaboration [1], a plethora of charmonium-like states have been reported, triggering the interest of the hadronic community (see some recent reviews in [2–6]). Among them, the recently discovered  $T_{cc}(3875)^+$  [7, 8] is taking a prominent role. Observed in the  $D^0D^0\pi^+$  mass distribution, this state has a mass of  $m_{\text{thr}} + \delta m_{\text{exp}}$ , with  $m_{\text{thr}} = 3875.09$  MeV being the  $D^{*+}D^0$  mass threshold and  $\delta m_{\text{exp}} = -360 \pm 40_{-0}^{+4}$  keV, whereas its width is  $\Gamma = 48 \pm 2_{-14}^{+0}$  keV [9].

From the theoretical perspective, there has been an extensive discussion on the nature of the  $T_{cc}(3875)^+$  state. On the one hand, several works advocate for the molecular interpretation of this state [5, 10–32] due to its proximity to the  $D^0D^{*+}$  and  $D^+D^{*0}$  thresholds. On the other hand, the tetraquark description has been assumed, even before its discovery [33–38]. However, the proximity to the  $D^0D^{*+}$  and  $D^+D^{*0}$  thresholds leads to considering hadronic degrees of freedom for the correct analysis of the experimental data [39, 40].

Given the interest in the  $T_{cc}(3875)^+$  state, ongoing work aims to identify scenarios in which its nature and properties can manifest more clearly. Recent efforts have been made to generate and understand the nature of the  $T_{cc}(3875)^+$  state using lattice QCD results [29, 41–46]. Also, work on femtoscopic correlation functions has been recently performed for the  $T_{cc}(3875)^+$  state in Refs. [47–49].

Another possible way to learn about the nature of the  $T_{cc}(3875)^+$  is to analyze its behavior under the extreme conditions of density and/or temperature present at Relativistic Heavy Ion Collider (RHIC), Large Hadron Collider (LHC) or the future Facility for Antiproton and Ion Research (FAIR) energies. In Ref. [50], the production of exotic tetraquarks, such as  $T_{QQ}$  with  $Q = c, b$ , was investigated using the quark coalescence model for Pb+Pb collisions at the LHC, showing production yields one order of magnitude smaller than previous estimates. In Ref. [51], the centrality dependence, rapidity, transverse momentum and elliptic flow in Pb+Pb for LHC energies for  $T_{cc}(3875)^+$  (as well as its potential isospin partners) were analyzed within the molecular picture using the AMPT transport model

\* Victor.Montesinos@ific.uv.es

† gmontana@jlab.org

‡ Miguel.Albaladejo@ific.uv.es

§ jmnieves@ific.uv.es

¶ tolos@ice.csic.es

including coalescence. The study found a strong enhancement of the  $T_{cc}$  yield in Pb+Pb collisions relative to  $pp$ , comparable to the  $X(3872)$  one in central collisions, while showing a considerably stronger decrease toward peripheral events. Also, in Ref. [52] the  $T_{cc}$  was investigated within the coalescence model in Pb+Pb at 5.02 TeV, concluding that it could either be a compact multi-quark configuration or a loosely bound molecular state composed of charmed mesons.

More recently, other production mechanisms have been proposed to understand the nature of this exotic state, such as photoproduction reactions involving one or two photons processes in ultra-peripheral collisions [53], prompt production of the  $T_{cc}^+$  (and its antimatter counterpart  $T_{\bar{c}\bar{c}}^-$ ) in  $pp$  collisions at a center-of-mass energy of 14 TeV [54], photoproduction off nuclei at near-threshold photon beam energies of 30–38 GeV that could be accessible in the proposed high-luminosity Electron-Ion Collider (EiC) and Electron-Ion Collider in China (EicC) [55], indirect production mechanisms through high-energy decay processes involving Higgs,  $Z_0$  and  $W^+$  at LHC or the Circular Electron-Positron Collider (CEPC) [56], and photoproduction via photon-gluon fusion at the International Linear Collider (ILC) and the Compact Linear Collider (CLIC) [57].

With the objective of analyzing the finite-density regime generated at the CBM experiment at FAIR, in Ref. [58] we have addressed the properties of  $T_{cc}(3875)^+$  and  $T_{\bar{c}\bar{c}}(3875)^-$  as well as their heavy-quark spin partners in nuclear matter, highlighting the distinctive density pattern of this particle-antiparticle pair if a small or a large molecular component in these tetraquark-like states was assumed.<sup>1</sup> In the present work, we aim to study the behavior of the  $T_{cc}(3875)^+$  and its heavy-quark spin partner  $T_{cc}(4016)^{++}$  at high temperatures, such as those produced at RHIC or LHC.

The  $T_{cc}(3875)^+$  and  $T_{cc}(4016)^{++}$  are generated as bound states from the interactions of the  $DD^*$  and  $D^*D^*$  mesons, respectively, assuming either a large or a small molecular component. The changes in the  $D$  and  $D^*$  propagators at finite temperature are implemented via the Imaginary-Time Formalism (ITF) so as to finally obtain the  $T_{cc}(3875)^+$  and  $T_{cc}(4016)^{++}$  thermal scattering amplitudes and spectral functions. The  $T_{\bar{c}\bar{c}}(3875)^-$  and  $T_{\bar{c}\bar{c}}(4016)^{-}$  at finite temperature behave similarly as  $T_{cc}(3875)^+$  and  $T_{cc}(4016)^{++}$ , respectively, given that the constituents  $\bar{D}$  and  $\bar{D}^*$  interact equally with a hot thermal bath of light mesons as the  $D$  and  $D^*$ .

The paper is organized as follows. In Sec. II we present the  $D^*D$  scattering amplitudes and the dynamical generation of the  $T_{cc}(3875)^+$  in free space and at finite temperature. We employ the ITF to obtain the two open-charm-meson thermal propagator, which determines the scattering amplitudes when the  $D$  and  $D^*$  mesons are immersed in the hot pion bath. In Sec. III we present our results for the  $T_{cc}(3875)^+$  (Subsec. III A), as well as for the  $T_{cc}^*(4016)^+$  (Subsec. III B). The main conclusions of our work are given in Sec. IV.

## II. FORMALISM

We start by considering the  $T_{cc}(3875)^+$  as an  $S$ -wave  $DD^*$  state with isospin and spin-parity quantum numbers  $I(J^P) = 0(1^+)$ . Following our previous works [58–60], we take into account two families of energy-dependent contact potentials, which are expanded around threshold as:

$$V_A(s) = C_1 + C_2 [s - (m_D + m_{D^*})^2], \quad (1a)$$

$$V_B(s) = (C'_1 + C'_2 [s - (m_D + m_{D^*})^2])^{-1}, \quad (1b)$$

where  $s = P^2$ , with  $P^\mu$  the total four-momentum of the  $DD^*$  pair. The quantities  $C_1^{(\prime)}$  and  $C_2^{(\prime)}$  are low-energy constants (LECs) that have to be adjusted, as we show in the following.

These interactions result from retaining the first two orders of the Taylor expansion around  $s = m_D + m_{D^*}$ , either of the potential  $V(s)$  (type  $A$ ) or of the inverse of the potential  $V^{-1}(s)$  (type  $B$ ). Note that the  $V_A(s)$  potential contains constant terms that give rise to purely molecular states as well as some contributions related to the exchange of genuine compact quark-model structures, whereas the  $V_B(s)$  is generated by the exchange of the bare quark-model  $T_{cc}(3875)^+$  state (see Ref. [58] for the discussion). With these potentials, we solve the Bethe-Salpeter Equation (BSE) for the  $T$ -matrix within the on-shell approximation [61],

$$\mathcal{T}^{-1}(s) = V^{-1}(s) - \Sigma_0(s), \quad (2)$$

<sup>1</sup> A dense nuclear medium induces also sizable charge-conjugation asymmetries in the  $D_{s0}^*(2317)^\pm$  and  $D_{s1}(2460)^\pm$  resonances, seen as isoscalar  $D^{(*)}K$  and  $\bar{D}^{(*)}\bar{K}$   $S$ -wave bound states, mainly due to the very different kaon and antikaon interactions with nuclear matter. In Ref. [59], we discussed in detail how this new feature can be used to better determine/limit the internal structure of these exotic states, similar to what was done in Ref. [58] for the  $T_{cc}(3875)^+$  and  $T_{\bar{c}\bar{c}}(3875)^-$ .

where  $\Sigma_0(s)$  is the  $DD^*$  loop function in the vacuum given by

$$\Sigma_0(s) = i \int \frac{d^4 q}{(2\pi)^4} \Delta_D(P - q) \Delta_{D^*}(q), \quad (3)$$

$$\Delta_{D,D^*}(q) = \frac{1}{(q^0)^2 - \vec{q}^2 - m_{D,D^*}^2 + i\varepsilon}, \quad (4)$$

which requires introducing an ultraviolet (UV) regulator in the  $d^3 q$  integration to make the two-point function  $\Sigma_0(s)$  finite. In this work, we will use a sharp momentum cutoff,  $\Lambda = 0.7$  GeV, as previously done in Refs. [58, 59].

To determine the LECs of the  $DD^*$  potential, we impose that the  $T_{cc}(3875)^+$  state appears in the vacuum as a pole in the first Riemann sheet of the BSE amplitude with

$$\mathcal{T}^{-1}(m_0^2) = 0, \quad \frac{d\mathcal{T}^{-1}(s)}{ds} \Big|_{s=m_0^2} = \frac{1}{g_0^2} = -\frac{1}{P_0} \frac{\partial \Sigma_0(s)}{\partial s} \Big|_{s=m_0^2}, \quad (5)$$

where  $m_0$  is the mass of the  $T_{cc}(3875)^+$ . We take its value to be 0.8 MeV below the isospin-symmetric  $DD^*$  threshold. This value is consistent with the analysis of Ref. [20]. In the last condition [62], we relate the coupling  $g_0$  of the two-hadron pair with the derivative of the loop function at the pole position and the molecular probability content  $P_0$  [63] (see also Ref. [30]). Therefore, we obtain expressions for  $V_A(s)$  and  $V_B(s)$  in terms of  $m_0$ ,  $\Sigma_0(m_0^2)$  and the derivative  $\Sigma'_0(m_0^2)$ . Similarly, we can obtain the  $V$ -potentials,  $T$ -matrices and  $D^*D^*$  loop functions for the  $T_{cc}(4016)^{**}$  state, the heavy-quark partner of the  $T_{cc}(3875)^+$ , by substituting  $D$  by  $D^*$  in the expressions above.

Once the LECs of the potential have been determined, we compute the finite-temperature scattering amplitude by considering temperature corrections on the  $D^*D^{(*)}$  loop function. We consider again the BSE equation for the  $T$ -matrix at temperature  $T$  as

$$\mathcal{T}^{-1}(E, \vec{P}; T) = V^{-1}(s) - \Sigma(E, \vec{P}; T), \quad (6)$$

where  $\Sigma(E, \vec{P}; T)$  is the temperature-dependent  $D^*D^{(*)}$  loop and  $s = E^2 - \vec{P}^2$ . The interaction kernel  $V(s)$  is taken the same as in free space.

In order to compute the finite-temperature corrections to the  $D^*D^{(*)}$  loop functions, we make use of the ITF to obtain the expression for the thermal propagator as

$$\begin{aligned} \Sigma(E, \vec{P}; T) = \int \frac{d^3 q}{(2\pi)^3} \int_0^\infty d\omega \int_0^\infty d\omega' \left\{ [1 + f(\omega, T) + f(\omega', T)] \left[ \frac{S_{M_1}(\omega, \vec{q}) S_{M_2}(\omega', \vec{P} - \vec{q})}{E - \omega - \omega' + i\varepsilon} - \frac{S_{\bar{M}_1}(\omega, \vec{q}) S_{\bar{M}_2}(\omega', \vec{P} - \vec{q})}{E + \omega + \omega' + i\varepsilon} \right] \right. \\ \left. + [f(\omega, T) - f(\omega', T)] \left[ \frac{S_{\bar{M}_1}(\omega, \vec{q}) S_{M_2}(\omega', \vec{P} - \vec{q})}{E + \omega - \omega' + i\varepsilon} - \frac{S_{M_1}(\omega, \vec{q}) S_{\bar{M}_2}(\omega', \vec{P} - \vec{q})}{E - \omega + \omega' + i\varepsilon} \right] \right\}, \quad (7) \end{aligned}$$

where  $f(\omega, T) = 1/(e^{\omega/T} - 1)$  is the Bose-Einstein distribution factor that appears from the summation over Matsubara frequencies within the ITF. The spectral functions  $S_{M_i}(\omega, \vec{q}; T)$ , with  $M_i$  being either  $D$  or  $D^*$ , consider the dressing of the heavy meson by the thermal medium. In this case, we employ the spectral functions for the  $D$  and  $D^*$  mesons obtained in Refs. [64, 65] from the interaction of the heavy mesons with a thermal bath of pions. We note that the spectral functions at finite temperature of  $D^{(*)}$  and  $\bar{D}^{(*)}$  are the same, given that the interaction of  $\bar{D}^{(*)}$ -mesons with light mesons is independent of whether the heavy meson is the particle or antiparticle. As can be observed in the left panels of Figs. 6 and 7 of Ref. [65], the thermal bath produces a large broadening of the spectral functions already at  $T = 80$  MeV.

We will compute the loop function at  $\vec{P} = 0$ . Using the fact that the spectral functions are the same for particle and antiparticle at finite temperature, we can simplify the previous expression of Eq. (7) as

$$\begin{aligned} \Sigma(E, \vec{P} = 0; T) = \int \frac{d^3 q}{(2\pi)^3} \int_0^\infty d\omega \int_0^\infty d\omega' S_{M_1}(\omega, |\vec{q}|) S_{M_2}(\omega', |\vec{q}|) \\ \times \left\{ [1 + f(\omega, T) + f(\omega', T)] \left( \frac{1}{E - \omega - \omega' + i\varepsilon} - \frac{1}{E + \omega + \omega' + i\varepsilon} \right) \right. \\ \left. + [f(\omega, T) - f(\omega', T)] \left( \frac{1}{E + \omega - \omega' + i\varepsilon} - \frac{1}{E - \omega + \omega' + i\varepsilon} \right) \right\}. \quad (8) \end{aligned}$$

From this formula, the imaginary part yields (integrating with respect to  $\omega'$ )

$$\begin{aligned} \text{Im } \Sigma(E, \vec{P} = 0; T) = & -\pi \int \frac{d^3 q}{(2\pi)^3} \int_0^\infty d\omega \int_0^\infty d\omega' S_{M_1}(\omega, |\vec{q}|) S_{M_2}(\omega', |\vec{q}|) \\ & \times \left\{ [1 + f(\omega, T) + f(\omega', T)] \text{sign}(E) \left[ \delta(\omega' - (E - \omega)) - \delta(\omega' + (E + \omega)) \right] \right. \\ & \left. + [f(\omega, T) - f(\omega', T)] \text{sign}(E) \left[ \delta(\omega' - (E + \omega)) - \delta(\omega' + (E - \omega)) \right] \right\}. \quad (9) \end{aligned}$$

If we set  $E > 0$ , then the second delta  $\delta(\omega' + E + \omega)$  will never give a contribution, as its argument will never become zero. Then, the expression gets simplified to

$$\begin{aligned} \text{Im } \Sigma(E > 0, \vec{P} = 0; T) = & -\frac{1}{2\pi} \int q^2 dq \\ & \times \left\{ \int_0^E d\omega S_{M_1}(\omega, |\vec{q}|) S_{M_2}(E - \omega, |\vec{q}|) [1 + f(\omega, T) + f(E - \omega, T)] \right. \\ & + \int_0^\infty d\omega S_{M_1}(\omega, |\vec{q}|) S_{M_2}(E + \omega, |\vec{q}|) [f(\omega, T) - f(E + \omega, T)] \\ & \left. - \int_E^\infty d\omega S_{M_1}(\omega, |\vec{q}|) S_{M_2}(\omega - E, |\vec{q}|) [f(\omega, T) - f(\omega - E, T)] \right\}. \quad (10) \end{aligned}$$

Note that the imaginary part is not UV divergent, whereas the real part is cutoff-dependent.

Having determined the loop function at finite temperature and, hence, the unitarized thermal scattering amplitude  $\mathcal{T}(E, \vec{P}; T)$ , the corresponding spectral function at finite temperature can be defined as

$$\mathcal{S}(E, \vec{P} = 0; T) = -\frac{1}{\pi} \text{Im } \mathcal{T}(E, \vec{P} = 0; T). \quad (11)$$

For hadronic ground states, the definition of the spectral function is related to the imaginary part of the propagator. This, however, is not possible for a purely dynamically generated state, where no preexisting asymptotic state exists. That is why one takes the  $DD^*$  scattering amplitude instead, as was done in the work of Ref. [66]. One can show that, in the case where we take the  $V_B$  potential, which includes an explicit exchange of a bare  $T_{cc}$  pole, the results for the spectral function stemming from Eq. (11) and from the usual definition in terms of the renormalized propagator are equivalent up to a normalization factor. This is not the case for the  $V_A$  potential, where, depending on the value taken for the molecular probability  $P_0$ , both definitions of the spectral function are only similar in an energy region around the vacuum mass of the  $T_{cc}$ .

### III. RESULTS

#### A. The $T_{cc}(3875)^+$ state

We start by showing the thermal  $DD^*$  loop function at finite temperature in Fig. 1. The real part of the loop function is calculated from Eq. (8) with a cutoff regularization of  $\Lambda = 0.7 \text{ GeV}$ , as previously mentioned, while the imaginary part follows directly from Eq. (10). For the computation of the real and imaginary parts of the  $DD^*$  loop function at finite temperature, we have used the spectral functions of the  $D$  and  $D^*$  obtained in Refs. [64, 65], as explained in Sec. II. In these references, it was determined that the thermal masses decrease as the temperature increases, while their widths grow substantially with temperature. Apart from the mass shift and the broadening, the spectral functions show little structure, especially when compared with the rich behavior exhibited by the finite nuclear-density ones used in Ref. [58] (see Figs. 6 and 7 of Ref. [65]).

As a consequence of the thermal modifications to the  $D^{(*)}$  mesons, the dressing of the loop functions with the  $D^{(*)}$  spectral functions softens and shifts towards lower energies the onset of the unitary cut of the imaginary part with

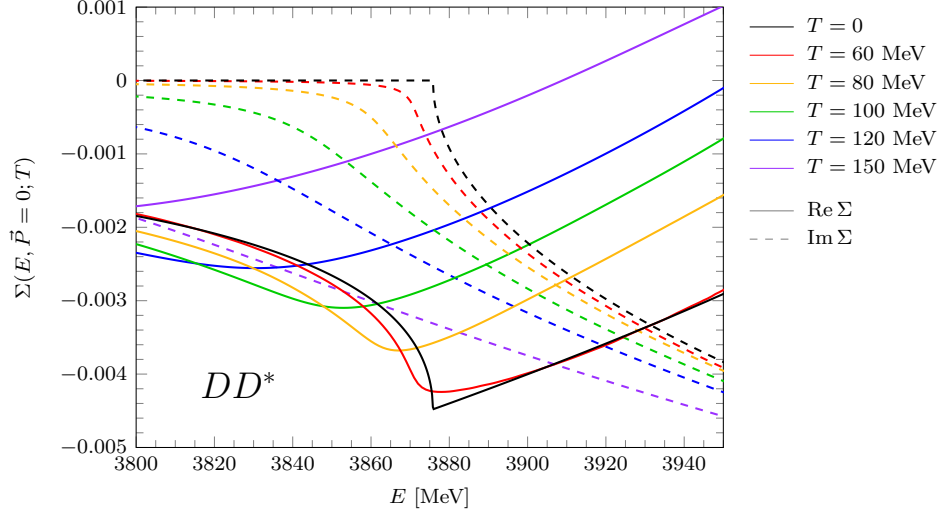


FIG. 1. Real (solid) and imaginary (dashed) parts of the  $DD^*$  loop function at several temperatures, ranging from  $T = 0$  MeV to  $T = 150$  MeV.

increasing temperature (dashed lines). The real part (solid lines) changes with temperature accordingly, with the cusp at the  $DD^*$  threshold lowering at larger temperatures. The real part also becomes less attractive with increasing temperature for energies larger than the threshold. We note that the behavior of the imaginary part of the  $DD^*$  loop with energy and temperature is the same as the one reported for  $D\bar{D}^*$  in Fig. 2 of Ref. [66], as expected. The real part behaves similarly with energy and temperature, although the exact values depend on the chosen regularization scale, which was different in the work of Ref. [66].

Once we have obtained the temperature-dependent  $DD^*$  loop functions  $\Sigma(E, \vec{P}; T)$ , the  $DD^*$   $T$ -matrices and the corresponding  $T_{cc}(3875)^+$  spectral functions ( $S_{T_{cc}}$ ) at finite temperature can be calculated from Eqs. (6) and (11), respectively. In Fig. 2 we show the spectral functions considering the two families of potentials,  $V_A$  (upper row) and  $V_B$  (lower row) for molecular probabilities  $P_0 = 0.2$  (left column) and 0.8 (right column). For each plot, we show the  $S_{T_{cc}}$  for different temperatures, ranging from  $T = 60$  MeV to  $T = 150$  MeV, close to the temperature of the QCD phase transition to quark matter.

If we compare the  $S_{T_{cc}}$  computed using the  $V_A$  potential and the ones obtained from the  $V_B$  potential, we find that for high values of the molecular  $DD^*$  component (right column) the results for both potentials are almost identical for all temperatures. As discussed in Refs. [58, 60], the zero of  $V_A$  and the bare pole of  $V_B$  are far from the energies considered to induce any significant changes. For the small value of  $P_0 = 0.2$  (left column), both potentials show significant deviations from each other, leading to different  $T$ -matrices at finite temperature, although both potentials give the same  $T_{cc}(3875)^+$  mass and  $DD^*$  coupling at zero temperature. A similar behavior was observed when the  $T_{cc}(3875)^+$  exotic state was embedded in a dense medium [58].

As for the temperature dependence for small and large  $P_0$ , we find that the spectral functions  $S_{T_{cc}}$  change more rapidly with temperature for high molecular probabilities. For large values of  $P_0$  (right column), the width increases significantly with temperature, leading to the melting of the  $T_{cc}(3875)^+$  for temperatures larger than 80 MeV. As for a small molecular component of  $P_0 = 0.2$  (left column), the changes in the spectral function due to temperature become less important, differing according to the potential used, as already indicated before. More precisely, the spectral functions obtained with  $V_A$  show the zero that this type of potential has, and vary with temperature above and below this zero, as already seen in the case of finite density in Ref. [58]. For the case of the  $V_B$  interaction, the quasi-particle peak, induced by the bare pole present in the potential, moves to higher energies while slowly melting down with temperature, in contrast to the case of large  $P_0$ . All these results indicate that any experimental determination of the scattering amplitudes at finite temperature can provide valuable insights into the molecular structure of the  $T_{cc}(3875)^+$  exotic state.

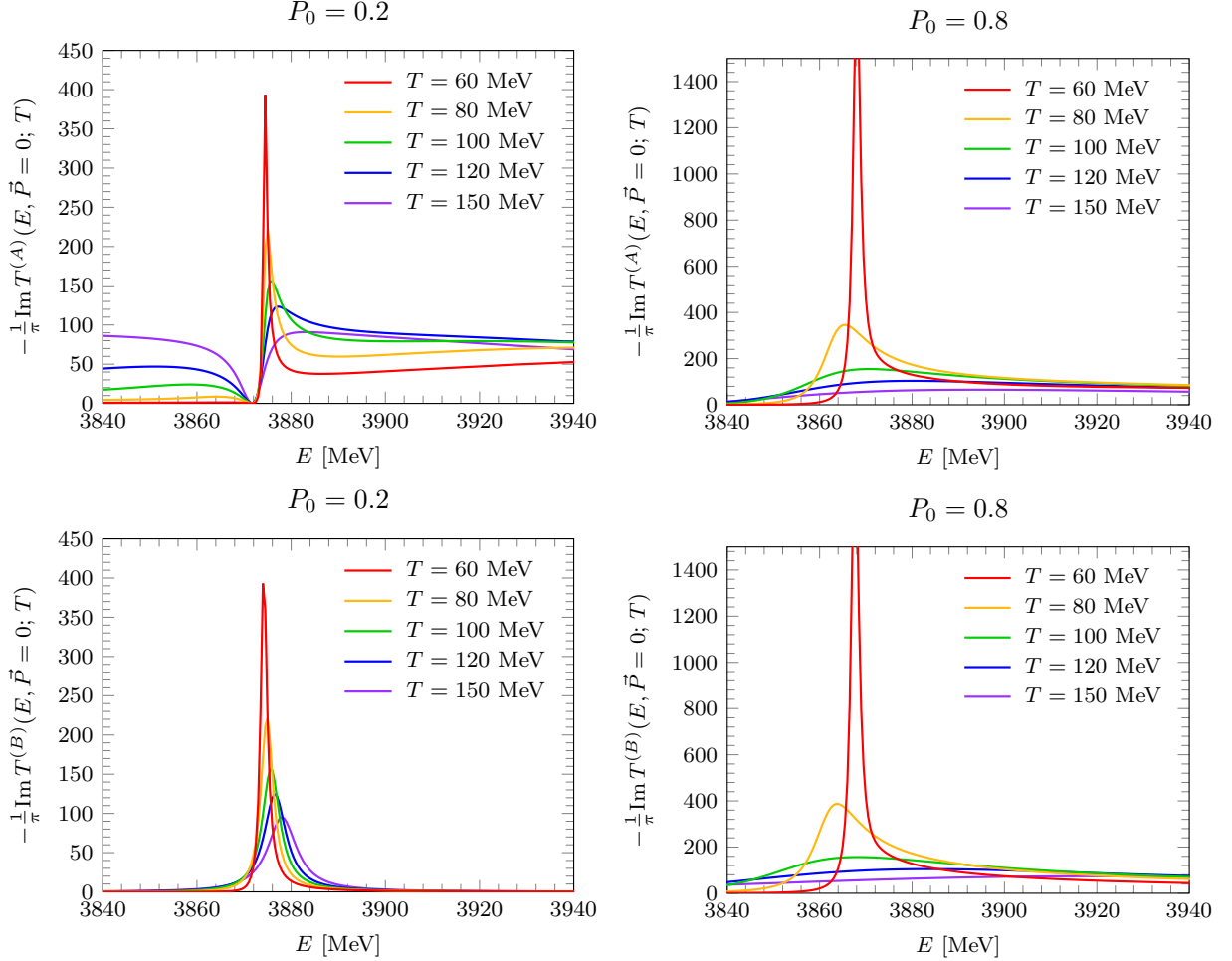


FIG. 2.  $T_{cc}$  spectral functions as a function of energy for different temperatures, computed using  $V_A$  [top row, cf. Eq. (1a)] and  $V_B$  [bottom row, cf. Eq. (1b)], for two values of the molecular probability (left and right columns).

### B. The HQSS partner of the $T_{cc}(3875)^+$ : the $T_{cc}(4016)^{++}$ state

Owing to Heavy Quark Spin Symmetry (HQSS), the  $T_{cc}$  has a plausible symmetric partner in the  $I(J^P) = 0(1^+)$   $D^*D^*$  channel. We will refer to this state as  $T_{cc}(4016)^{++}$ , or, for brevity,  $T_{cc}^*$ . This state has been studied in several theoretical works [20, 21, 58, 67]. In Fig. 3 we present the results for the  $D^*D^*$  loop function. Similarly to the case of the  $DD^*$  loop, we also use a cutoff regulator  $\Lambda = 0.7$  GeV for the evaluation of its real part. The obtained results are qualitatively similar to those of the  $DD^*$  loop, but shifting the opening of the unitarity cut by the appropriate mass difference  $m_{D^*} - m_D \approx m_\pi$ . As in the  $DD^*$  case, we can observe a general softening and shift towards lower energies of the onset of the unitarity cut, in both the real (solid lines) and imaginary (dashed lines) parts. This is again due to the decrease in the thermal mass of the  $D^*$  mesons found in Refs. [64, 65]. One can observe in the  $D^*D^*$  case a slightly less attractive real part, as compared with the real part of the  $DD^*$  loop. Conversely, the imaginary part is also slightly larger. However, these differences are not very notable.

Given that the  $I(J^P) = 0(1^+)$   $DD^*$  and  $D^*D^*$  interaction kernels are the same due to HQSS, the  $T_{cc}^*$  state is predicted to have a binding energy similar to that of the  $T_{cc}$ , now taken with respect to the  $D^*D^*$  threshold. Actually, the  $T_{cc}^*$  is expected to be slightly more bound than the  $T_{cc}$ , owing to the modification of the kinetic term of the  $D^*D^*$  channel. In our approach, we take two different values for the binding energy, defined as

$$E_b = 2m_{D^*} - m_0^{T_{cc}^*}, \quad (12)$$

so as to analyze the effect of this parameter on the lineshape of the  $T_{cc}^*$  spectral function  $S_{T_{cc}^*}$ . The results for the  $T_{cc}^*$  spectral functions can be found in the plots of Fig. 4. We plot  $S_{T_{cc}^*}$  derived from the  $V_B$  interaction, for several values



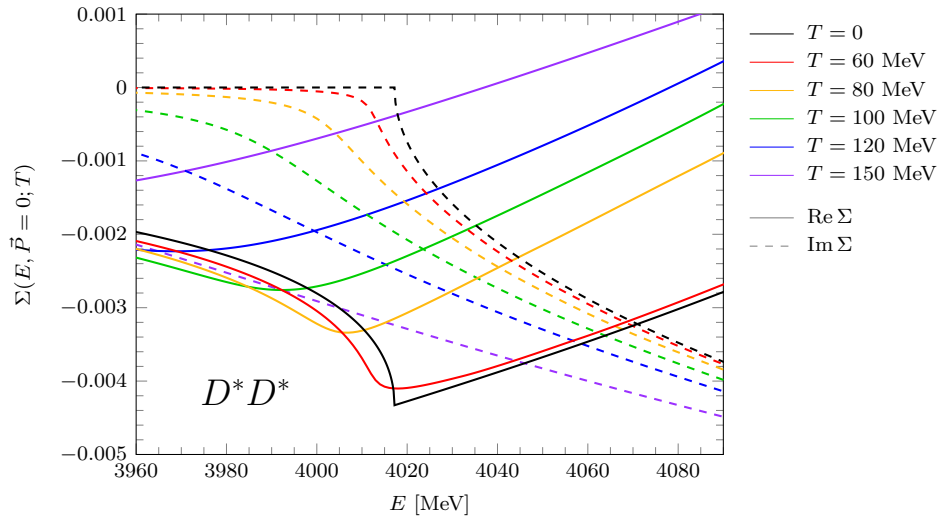


FIG. 3. Real (solid) and imaginary (dashed) parts of the  $D^*D^*$  loop function at several temperatures, ranging from  $T = 0$  MeV to  $T = 150$  MeV.

of the temperature, and considering the same two molecular probabilities as in the case of the  $T_{cc}$ . A comparison with the results obtained when using the  $V_A$  potential will be redundant with what has already been discussed for the  $T_{cc}$ . The top row is computed using a binding energy  $E_b = 0.8$  MeV, while in the bottom row the value  $E_b = 2.0$  MeV has been used. In Ref. [20], the binding of the  $T_{cc}^*$  with respect to the  $D^{*+}D^{*0}$  threshold was predicted to be around  $1.2 \sim 1.6$  MeV, depending on the regularization scale chosen. These values are included in the range of binding energies that we consider.

When comparing the results obtained here for the  $T_{cc}^*$  with those shown in Fig. 2 for the  $T_{cc}$ , we observe a similar qualitative behavior. This was also the case in Ref. [66], when comparing the temperature effects on the  $X(3872)$  and its  $2^{++}$  heavy quark spin partner  $X(4014)$  (see Fig. 3 in that reference). In the study of Ref. [58] of the  $T_{cc}$  and  $T_{cc}^*$  in the presence of a dense nuclear medium, a similar qualitative behavior with density was also found for the two HQSS partners. In the plots of Fig. 4, we see that the  $T_{cc}^*$  spectral functions are more affected by the hot bath in the high molecular probability scenario. When comparing the  $E_b = 2$  MeV and  $0.8$  MeV scenarios, we note a slight narrowing of the state, most visible in the  $P_0 = 0.8$ ,  $T = 80$  MeV. This is to be expected, given the larger binding energy. However, the strong melting of the  $T_{cc}^*$  is still noticeable at temperatures around  $100$  MeV, and is almost not affected by the variation of the binding energy in the considered range.

#### IV. CONCLUSIONS

We have discussed the spectral properties of the tetraquark-like  $T_{cc}(3875)^+$  and  $T_{cc}(4016)^{*+}$  immersed in a hot bath of pions. We have considered these exotic states as purely isoscalar  $DD^*$  and  $D^*D^*$   $S$ -wave bound states, respectively. For the BSE interaction kernel at zero temperature, we have considered two families of energy-dependent interactions that allow for a more exhaustive analysis of the molecular probability content of these states. The effects of finite temperature are incorporated up to  $T = 150$  MeV through the  $D^{(*)}$  thermal spectral functions calculated in Ref. [65], with the changes in the  $D^{(*)}$  propagators implemented using the ITF.

We have found important modifications of the  $D^*D^{(*)}$  scattering amplitudes already for  $T = 80$  MeV. They are produced by the dressing of the two open-charm-meson loop functions with the  $D$  and  $D^*$  spectral functions, which softens and shifts towards lower energies the onset of the unitary cut of the imaginary part with increasing temperature. The real part changes with temperature accordingly, with the cusp at the  $DD^*$  threshold lowering at larger temperatures. Next, we have discussed the dependence of the hot-bath lineshapes of these tetraquark-like states on their Weinberg molecular content, and found that the  $S_{T_{cc}^{(*)}}$  spectral functions change more rapidly with temperature for high molecular probabilities. For large values of  $P_0$ , the widths significantly increase with temperature, leading to the melting of these exotic states for temperatures larger than  $80$  MeV. For small molecular components, the changes in the spectral functions of these states due to temperature become less important, and depend significantly

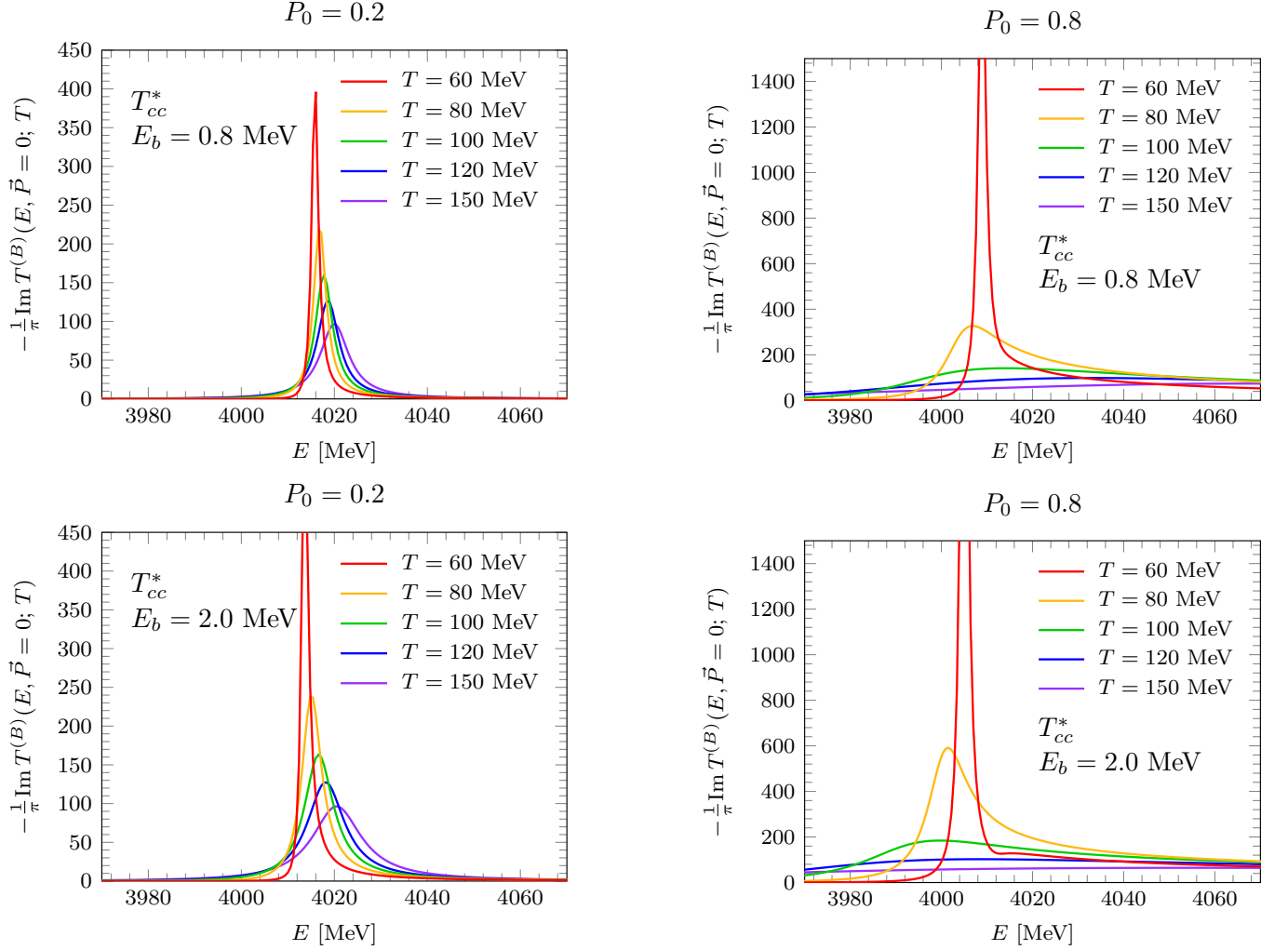


FIG. 4.  $T_{cc}(4016)^{++}$  spectral functions as a function of energy for different temperatures, computed using  $V_B$  [cf. Eq. (1b)], for two values of the molecular probability (left and right columns, respectively), and two different binding energies (top and bottom rows).

on the employed BSE potential kernel.

These results show that any experimental determination of the  $D^{(*)}D^*$  scattering amplitudes at finite temperature, in experiments like RHIC or LHC, will provide valuable insights into the molecular structure of the  $T_{cc}(3875)^+$  and  $T_{cc}(4016)^{++}$  states. Furthermore, by combining the thermal line-shape patterns of these states with future measurements at FAIR (CBM, PANDA) of their spectral properties in dense nuclear environments [58], as well as those of their antiparticles, it should be possible to very efficiently constrain the nature of these enigmatic tetraquark-like exotics.

## ACKNOWLEDGMENTS

We acknowledge support from the programs Unidades de Excelencia Severo Ochoa CEX2023-001292-S and María de Maeztu CEX2020-001058-M, from the projects PID 2020-112777GB-I00, PID2022-139427NB-I00 and PID2023-147458NB-C21 financed by the Spanish MCIN/AEI/10.13039/501100011033, as well as from the Grant CIPROM 2023/59 of Generalitat Valenciana, the Generalitat de Catalunya under contract 2021 SGR 171, and by the CRC-TR 211 'Strong-interaction matter under extreme conditions'-project Nr. 315477589 - TRR 211. M. A. acknowledges financial support through GenT program by Generalitat Valencia (GVA) Grant No. CIDEAGENT/2020/002, Ramón



y Cajal program by MICINN Grant No. RYC2022-038524-I, and “Atracción de Talento” program by CSIC, Grant No. PIE 20245AT019. G.M. was supported by the U.S. Department of Energy contract DE-AC05-06OR23177, under which Jefferson Science Associates, LLC operates Jefferson Lab. V.M. acknowledges support by GVA under Grant No. ACIF/2021/290.

- 
- [1] BELLE collaboration, *Observation of a narrow charmonium-like state in exclusive  $B^\pm \rightarrow K^\pm \pi^+ \pi^- J/\psi$  decays*, *Phys. Rev. Lett.* **91** (2003) 262001 [[hep-ex/0309032](#)].
  - [2] F.-K. Guo, C. Hanhart, U.-G. Meißner, Q. Wang, Q. Zhao and B.-S. Zou, *Hadronic molecules*, *Rev. Mod. Phys.* **90** (2018) 015004 [[1705.00141](#)].
  - [3] Y.-R. Liu, H.-X. Chen, W. Chen, X. Liu and S.-L. Zhu, *Pentaquark and Tetraquark states*, *Prog. Part. Nucl. Phys.* **107** (2019) 237 [[1903.11976](#)].
  - [4] N. Brambilla, S. Eidelman, C. Hanhart, A. Nefediev, C.-P. Shen, C.E. Thomas et al., *The XYZ states: experimental and theoretical status and perspectives*, *Phys. Rept.* **873** (2020) 1 [[1907.07583](#)].
  - [5] X.-K. Dong, F.-K. Guo and B.-S. Zou, *A survey of heavy-heavy hadronic molecules*, *Commun. Theor. Phys.* **73** (2021) 125201 [[2108.02673](#)].
  - [6] H.-X. Chen, W. Chen, X. Liu, Y.-R. Liu and S.-L. Zhu, *An updated review of the new hadron states*, *Rept. Prog. Phys.* **86** (2023) 026201 [[2204.02649](#)].
  - [7] LHCb collaboration, *A model-independent study of resonant structure in  $B^+ \rightarrow D^+ D^- K^+$  decays*, *Phys. Rev. Lett.* **125** (2020) 242001 [[2009.00025](#)].
  - [8] LHCb collaboration, *Amplitude analysis of the  $B^+ \rightarrow D^+ D^- K^+$  decay*, *Phys. Rev. D* **102** (2020) 112003 [[2009.00026](#)].
  - [9] LHCb collaboration, *Study of the doubly charmed tetraquark  $T_{cc}^+$* , *Nature Commun.* **13** (2022) 3351 [[2109.01056](#)].
  - [10] D. Janc and M. Rosina, *The  $T_{cc} = DD^*$  molecular state*, *Few Body Syst.* **35** (2004) 175 [[hep-ph/0405208](#)].
  - [11] T.F. Carames, A. Valcarce and J. Vijande, *Doubly charmed exotic mesons: A gift of nature?*, *Phys. Lett. B* **699** (2011) 291.
  - [12] S. Ohkoda, Y. Yamaguchi, S. Yasui, K. Sudoh and A. Hosaka, *Exotic mesons with double charm and bottom flavor*, *Phys. Rev. D* **86** (2012) 034019 [[1202.0760](#)].
  - [13] N. Li, Z.-F. Sun, X. Liu and S.-L. Zhu, *Coupled-channel analysis of the possible  $D^{(*)}D^{(*)}$ ,  $\bar{B}^{(*)}\bar{B}^{(*)}$  and  $D^{(*)}\bar{B}^{(*)}$  molecular states*, *Phys. Rev. D* **88** (2013) 114008 [[1211.5007](#)].
  - [14] M.-Z. Liu, T.-W. Wu, M. Pavon Valderrama, J.-J. Xie and L.-S. Geng, *Heavy-quark spin and flavor symmetry partners of the  $X(3872)$  revisited: What can we learn from the one boson exchange model?*, *Phys. Rev. D* **99** (2019) 094018 [[1902.03044](#)].
  - [15] A. Feijoo, W.H. Liang and E. Oset,  *$D0D0\pi^+$  mass distribution in the production of the  $T_{cc}$  exotic state*, *Phys. Rev. D* **104** (2021) 114015 [[2108.02730](#)].
  - [16] X.-Z. Ling, M.-Z. Liu, L.-S. Geng, E. Wang and J.-J. Xie, *Can we understand the decay width of the  $T_{cc}^+$  state?*, *Phys. Lett. B* **826** (2022) 136897 [[2108.00947](#)].
  - [17] S. Fleming, R. Hodges and T. Mehen,  *$T_{cc}^+$  decays: Differential spectra and two-body final states*, *Phys. Rev. D* **104** (2021) 116010 [[2109.02188](#)].
  - [18] H. Ren, F. Wu and R. Zhu, *Hadronic Molecule Interpretation of  $T_{cc}^+$  and Its Beauty Partners*, *Adv. High Energy Phys.* **2022** (2022) 9103031 [[2109.02531](#)].
  - [19] K. Chen, R. Chen, L. Meng, B. Wang and S.-L. Zhu, *Systematics of the heavy flavor hadronic molecules*, *Eur. Phys. J. C* **82** (2022) 581 [[2109.13057](#)].
  - [20] M. Albaladejo,  *$T_{cc}^+$  coupled channel analysis and predictions*, *Phys. Lett. B* **829** (2022) 137052 [[2110.02944](#)].
  - [21] M.-L. Du, V. Baru, X.-K. Dong, A. Filin, F.-K. Guo, C. Hanhart et al., *Coupled-channel approach to  $T_{cc}^+$  including three-body effects*, *Phys. Rev. D* **105** (2022) 014024 [[2110.13765](#)].
  - [22] V. Baru, X.-K. Dong, M.-L. Du, A. Filin, F.-K. Guo, C. Hanhart et al., *Effective range expansion for narrow near-threshold resonances*, *Phys. Lett. B* **833** (2022) 137290 [[2110.07484](#)].
  - [23] N. Santowsky and C.S. Fischer, *Four-quark states with charm quarks in a two-body Bethe–Salpeter approach*, *Eur. Phys. J. C* **82** (2022) 313 [[2111.15310](#)].
  - [24] C. Deng and S.-L. Zhu,  *$T_{cc}^+$  and its partners*, *Phys. Rev. D* **105** (2022) 054015 [[2112.12472](#)].
  - [25] H.-W. Ke, X.-H. Liu and X.-Q. Li, *Possible molecular states of  $D^{(*)}D^{(*)}$  and  $B^{(*)}B^{(*)}$  within the Bethe–Salpeter framework*, *Eur. Phys. J. C* **82** (2022) 144 [[2112.14142](#)].
  - [26] S.S. Agaev, K. Azizi and H. Sundu, *Hadronic molecule model for the doubly charmed state  $T_{cc}^+$* , *JHEP* **06** (2022) 057 [[2201.02788](#)].
  - [27] L. Meng, B. Wang, G.-J. Wang and S.-L. Zhu, *Chiral perturbation theory for heavy hadrons and chiral effective field theory for heavy hadronic molecules*, *Phys. Rept.* **1019** (2023) 1 [[2204.08716](#)].
  - [28] L.M. Abreu, *A note on the possible bound  $D^{(*)}D^{(*)}$ ,  $B^{-(*)}B^{-(*)}$  and  $D^{(*)}B^{-(*)}$  states*, *Nucl. Phys. B* **985** (2022) 115994 [[2206.01166](#)].
  - [29] S. Chen, C. Shi, Y. Chen, M. Gong, Z. Liu, W. Sun et al.,  *$T_{cc}^+(3875)$  relevant  $DD^*$  scattering from  $N_f = 2$  lattice QCD*, *Phys. Lett. B* **833** (2022) 137391 [[2206.06185](#)].

- [30] M. Albaladejo and J. Nieves, *Compositeness of S-wave weakly-bound states from next-to-leading order Weinberg's relations*, *Eur. Phys. J. C* **82** (2022) 724 [2203.04864].
- [31] L.R. Dai, L.M. Abreu, A. Feijoo and E. Oset, *The isospin and compositeness of the  $T_{cc}(3875)$  state*, *Eur. Phys. J. C* **83** (2023) 983 [2304.01870].
- [32] G.-J. Wang, Z. Yang, J.-J. Wu, M. Oka and S.-L. Zhu, *New insight into the exotic states strongly coupled with the  $D\bar{D}^*$  from the  $T_{cc}^+$* , *Sci. Bull.* **69** (2024) 3036 [2306.12406].
- [33] J.L. Ballot and J.M. Richard, *FOUR QUARK STATES IN ADDITIVE POTENTIALS*, *Phys. Lett. B* **123** (1983) 449.
- [34] S. Zouzou, B. Silvestre-Brac, C. Gignoux and J.M. Richard, *FOUR QUARK BOUND STATES*, *Z. Phys. C* **30** (1986) 457.
- [35] F.S. Navarra, M. Nielsen and S.H. Lee, *QCD sum rules study of  $QQ$  - anti-u anti-d mesons*, *Phys. Lett. B* **649** (2007) 166 [hep-ph/0703071].
- [36] D. Ebert, R.N. Faustov, V.O. Galkin and W. Lucha, *Masses of tetraquarks with two heavy quarks in the relativistic quark model*, *Phys. Rev. D* **76** (2007) 114015 [0706.3853].
- [37] M. Karliner and J.L. Rosner, *Discovery of doubly-charmed  $\Xi_{cc}$  baryon implies a stable  $(bb\bar{u}\bar{d})$  tetraquark*, *Phys. Rev. Lett.* **119** (2017) 202001 [1707.07666].
- [38] G. Yang, J. Ping and J. Segovia, *Doubly-heavy tetraquarks*, *Phys. Rev. D* **101** (2020) 014001 [1911.00215].
- [39] X.-K. Dong, F.-K. Guo and B.S. Zou, *Near Threshold Structures and Hadronic Molecules*, *Few Body Syst.* **62** (2021) 61.
- [40] L.R. Dai, J. Song and E. Oset, *Evolution of genuine states to molecular ones: The  $T_{cc}(3875)$  case*, *Phys. Lett. B* **846** (2023) 138200 [2306.01607].
- [41] M. Padmanath and S. Prelovsek, *Signature of a Doubly Charm Tetraquark Pole in  $DD^*$  Scattering on the Lattice*, *Phys. Rev. Lett.* **129** (2022) 032002 [2202.10110].
- [42] Y. Lyu, S. Aoki, T. Doi, T. Hatsuda, Y. Ikeda and J. Meng, *Doubly Charmed Tetraquark  $T_{cc}+$  from Lattice QCD near Physical Point*, *Phys. Rev. Lett.* **131** (2023) 161901 [2302.04505].
- [43] S. Collins, A. Nefediev, M. Padmanath and S. Prelovsek, *Toward the quark mass dependence of  $T_{cc}+$  from lattice QCD*, *Phys. Rev. D* **109** (2024) 094509 [2402.14715].
- [44] HADRON SPECTRUM collaboration, *Near-threshold states in coupled  $DD^*-D^*D^*$  scattering from lattice QCD*, *Phys. Rev. D* **111** (2025) 034511 [2405.15741].
- [45] M.-L. Du, A. Filin, V. Baru, X.-K. Dong, E. Epelbaum, F.-K. Guo et al., *Role of Left-Hand Cut Contributions on Pole Extractions from Lattice Data: Case Study for  $T_{cc}(3875)^+$* , *Phys. Rev. Lett.* **131** (2023) 131903 [2303.09441].
- [46] F. Gil-Domínguez, A. Giachino and R. Molina, *Quark mass dependence of the  $T_{cc}(3875)^+$  pole*, *Phys. Rev. D* **111** (2025) 016029 [2409.15141].
- [47] Y. Kamiya, T. Hyodo and A. Ohnishi, *Femtoscopic study on  $DD^*$  and  $D\bar{D}^*$  interactions for  $T_{cc}$  and  $X(3872)$* , *Eur. Phys. J. A* **58** (2022) 131 [2203.13814].
- [48] I. Vidana, A. Feijoo, M. Albaladejo, J. Nieves and E. Oset, *Femtoscopic correlation function for the  $T_{cc}(3875)^+$  state*, *Phys. Lett. B* **846** (2023) 138201 [2303.06079].
- [49] M. Albaladejo, A. Feijoo, I. Vidaña, J. Nieves and E. Oset, *Inverse problem in femtoscopic correlation functions: The  $T_{cc}(3875)^+$  state*, **2307.09873**.
- [50] C.E. Fontoura, G. Krein, A. Valcarce and J. Vijande, *Production of exotic tetraquarks  $QQ\bar{q}\bar{q}$  in heavy-ion collisions at the LHC*, *Phys. Rev. D* **99** (2019) 094037 [1905.03877].
- [51] Y. Hu, J. Liao, E. Wang, Q. Wang, H. Xing and H. Zhang, *Production of doubly charmed exotic hadrons in heavy ion collisions*, *Phys. Rev. D* **104** (2021) L111502 [2109.07733].
- [52] H. Yun, D. Park, S. Noh, A. Park, W. Park, S. Cho et al.,  *$X(3872)$  and  $T_{cc}$ : Structures and productions in heavy ion collisions*, *Phys. Rev. C* **107** (2023) 014906 [2208.06960].
- [53] X. Wang, Y. Xie, Y. Huang and X. Chen, *Exclusive production of  $T_{cc}$ - in hadron-hadron ultraperipheral collisions*, *Phys. Rev. D* **109** (2024) 016007 [2310.00980].
- [54] X.-L. Hua, Y.-Y. Li, Q. Wang, S. Yang, Q. Zhao and B.-S. Zou, *Revealing the mystery of the double charm tetraquark in  $pp$  collision*, *Eur. Phys. J. C* **84** (2024) 800 [2310.04258].
- [55] E.Y. Paryev, *An alternative way to decipher the nature of the doubly charmed tetraquark  $T_{cc}(3875)^+$ : Its antiparticle  $T_{\bar{c}\bar{c}}(3875)^-$  photoproduction off nuclei near threshold*, *Int. J. Mod. Phys. A* **39** (2024) 2450115 [2408.00360].
- [56] J.-J. Niu, B.-B. Shi, Z.-K. Tao and H.-H. Ma, *Indirect production of doubly charmed tetraquark  $T_{cc}$  at high energy colliders*, *Phys. Rev. D* **111** (2025) 014019 [2410.09322].
- [57] J.-J. Niu and H.-H. Ma, *Photoproduction of doubly charmed tetraquark  $T_{cc}$  via photon-gluon fusion at ILC and CLIC*, **2506.16721**.
- [58] V. Montesinos, M. Albaladejo, J. Nieves and L. Tolos, *Properties of the  $T_{cc}(3875)^+$  and  $T_{\bar{c}\bar{c}}(3875)^-$  and their heavy-quark spin partners in nuclear matter*, *Phys. Rev. C* **108** (2023) 035205 [2306.17673].
- [59] V. Montesinos, M. Albaladejo, J. Nieves and L. Tolos, *Charge-conjugation asymmetry and molecular content: The  $Ds0^*(2317)^\pm$  in matter*, *Phys. Lett. B* **853** (2024) 138656 [2403.00451].
- [60] M. Albaladejo, J.M. Nieves and L. Tolos,  *$DD^{\mp*}$  scattering and  $\chi c1(3872)$  in nuclear matter*, *Phys. Rev. C* **104** (2021) 035203 [2102.08589].
- [61] J. Nieves and E. Ruiz Arriola, *Bethe-Salpeter approach for unitarized chiral perturbation theory*, *Nucl. Phys. A* **679** (2000) 57 [hep-ph/9907469].
- [62] D. Gamermann, J. Nieves, E. Oset and E. Ruiz Arriola, *Couplings in coupled channels versus wave functions: application to the  $X(3872)$  resonance*, *Phys. Rev. D* **81** (2010) 014029 [0911.4407].
- [63] S. Weinberg, *Evidence That the Deuteron Is Not an Elementary Particle*, *Phys. Rev.* **137** (1965) B672.

- [64] G. Montaña, A. Ramos, L. Tolos and J.M. Torres-Rincon, *Impact of a thermal medium on  $D$  mesons and their chiral partners*, *Phys. Lett. B* **806** (2020) 135464 [[2001.11877](#)].
- [65] G. Montaña, A. Ramos, L. Tolos and J.M. Torres-Rincon, *Pseudoscalar and vector open-charm mesons at finite temperature*, *Phys. Rev. D* **102** (2020) 096020 [[2007.12601](#)].
- [66] G. Montaña, A. Ramos, L. Tolos and J.M. Torres-Rincon,  *$X(3872)$ ,  $X(4014)$ , and their bottom partners at finite temperature*, *Phys. Rev. D* **107** (2023) 054014 [[2211.01896](#)].
- [67] L.R. Dai, R. Molina and E. Oset, *Prediction of new  $T_{cc}$  states of  $D^*D^*$  and  $Ds^*D^*$  molecular nature*, *Phys. Rev. D* **105** (2022) 016029 [[2110.15270](#)].